energies

MDPI

Article

Numerical Investigation of the Adsorption Process of Zeolite/Water in a Thermochemical Reactor for Seasonal Heat Storage

Elham Abohamzeh * and Georg Frey

Automation and Energy Systems, Saarland University, 66123 Saarbrücken, Germany
* Correspondence: elham.abohamzeh@aut.uni-saarland.de

Abstract: Zeolite 13X molecular sieve with high sorption capacity and significant sorption rate has been considered a promising candidate for seasonal heat storage. In this study, a code is developed to simulate the adsorption process between zeolite and water in all ranges of partial pressures, temperatures, and sorbate loadings. The results from the proposed code were compared with experiments and good agreement was observed. After validation, the developed model was used to study the effective parameters involved in the adsorption process of binder-free Zeolite 13X. A parametric study considering various temperatures and water content in the inflow air was conducted and the influence of different factors on the outlet temperature and adsorption enthalpy has been studied. This parametric study gives a good insight into the measures which can be taken for achieving the desired released energy or having the outlet temperature in the preferred range. The simulations have been conducted in a variety of temperature ranges provided during the desorption process, the humidity amount, and the mass flow rate of the incoming air. The relative influence of each parameter in the specified ranges is presented. The results have demonstrated the direct relationship of the partial pressure of water vapor and the desorption temperature with the adsorbed water amount and adsorption enthalpy while changing the mass flow rate mostly influences the discharging time.

Keywords: thermochemical heat storage; adsorption process; zeolite; energy storage density; computational fluid dynamics

Citation: Abohamzeh, E.; Frey, G. Numerical Investigation of the Adsorption Process of Zeolite/Water in a Thermochemical Reactor for Seasonal Heat Storage. *Energies* **2022**, *15*, 5944. https://doi.org/10.3390/en15165944

Academic Editor: Lei Wang

Received: 24 July 2022
Accepted: 14 August 2022
Published: 17 August 2022

1. Introduction

There is a global aim to decrease energy consumption from fossil fuels considering their limited resources and environmental issues. To achieve this, the increasing use of renewable energy sources is necessary. Solar energy, basically known for its infinite and renewable nature, is one of the most widely used today. However, considering its variability and seasonal availability, the major challenge continues to be the need of storing this free source of energy for time periods with little solar radiation. The technology of thermochemical energy storage has been proposed as a promising approach for minimizing the temporal mismatch between heating demand and solar energy supply. In comparison to other thermal energy storage methods, the remarkable advantage of this technology is long-term energy preservation with negligible heat loss and high energy density. In these systems, the reversible process of desorption and adsorption makes it possible to store solar heat from summer to winter, so that the heat can be supplied to residential buildings with a very high proportion of solar energy.

Adsorption is the adhesion of an atom, ion, or molecule (adsorbate) to a surface of commonly a porous solid (adsorbent). A film of the adsorbate is created on the adsorbent surface in this process. The reverse process is called desorption. This phenomenon is a surface phenomenon since it occurs just on the solid surface and does not include the bulk of the solid material, like what is observed in the absorption process [1].

Different adsorption materials have been studied by researchers. Activated carbon, zeolite sieves, silica gel, and natural rocks are traditional physical sorbents [2,3]. Among them, zeolite sieves, which are aluminosilicate minerals of alkaline or alkali earth metals (calcium, sodium, and potassium) with a microporous structure for moisture adsorption, are one of the most used. They have regeneration temperatures in the range of 150–300 °C and high storage density. Until now there are more than 40 types of natural zeolites and more than 150 synthesized zeolites [4]. Zeolites 4A, 5A, 10X, and 13X are among the most used zeolites for sorption energy storage [5]. Among them, zeolite 13X with a maximum water adsorption capacity of 12–36% by mass [6,7] is known as the one with the most potential considering its large sorption capacity and high sorption rate. Compared with silica gel, which is another traditional sorbent, zeolite has a higher energy storage density; however, a higher regeneration temperature is required. A regeneration temperature of about 180–300 °C and adsorption enthalpy of about 3300–4200 kJ/kg have been reported for the zeolite–water pair by Wang et al. [8]. Zeolite 13X has various applications such as thermal storage [9] and sorption cooling [10,11]. High adsorption enthalpy of the zeolite/water pair in comparison with other adsorption pairs such as activated carbon/ammonia or silica gel/water make it a promising candidate for thermal storage applications.

The main objective of research in the area of sorption storage systems for buildings is to develop a reactor with the ability to provide adsorption heat at temperature levels suitable for space heating. A thermochemical (sorption) energy storage prototype for space heating was developed by [12] in the MonoSorp project framework. In this system, zeolite 4A honeycomb structures (70 kg) were utilized. During the experiments, a sorption temperature of about 20 °C and a regeneration temperature of 180 °C was used. Based on the experiments, in the system with an inlet air temperature of 19 °C and an inlet water vapor pressure of 8.7 mbar, they measured 22 °C as maximum temperature increase and discharging powers of 1–1.5 kW. Another prototype was developed by Jähnig et al. [13] with about 200 kg of silica gel. The experiments showed an energy density of about 50 kWh/m^3 for the materials and a temperature lift of only 5 K, revealing that silica gel has a very poor thermal conductivity and also that a very limited temperature increase can be achieved. The main conclusion claimed by the authors is that silica gel is not suitable for heat storage purposes. In an experimental study conducted by Hongois et al. [14], sorption experiments in a reactor filled with 200 g zeolite-$MgSO_4$ composites were carried out. They considered different relative humidities of air and mass flow rates. Their results demonstrated a high influence of relative humidity of air on the system operation.

The most investigated reactors are fixed-bed reactors. In these reactors, the sorbent is kept within the reactor, and both adsorption and desorption occur in the reactor. A reaction zone with relatively high temperatures is formed, which moves from the area of the steam inlet to the steam outlet [5]. In the COMTES project [9,15], zeolite 13XBF was used for seasonal heat storage purposes in buildings. They developed a fixed bed reactor with about 300 L and 164 kg of zeolite. Based on their results, an energy density of about 177 kWh/m^3 can be provided by this system.

Although experiments are required for the investigation of processes in sorption reactors, it is usually time-consuming and expensive to conduct several experiments to study the different involved parameters. Here, numerical studies can provide a more effective and cheaper way to investigate adsorption and desorption processes. Therefore, some numerical studies have been conducted to understand the process properly. Jänchen et al. [16] performed a CFD simulation to compare the performance of zeolite 4A pellet beds zeolite and 4A honeycombs with and without binder in the adsorption process. The results have shown the better performance of binder-free zeolite honeycombs, which might be due to the optimum secondary pore size distribution, leading to enhanced performance during the adsorption process.

The aim of the present work is to develop a one-dimensional code using computational fluid dynamics (CFD) to model the adsorption process of zeolite 13X and water in a fixed-bed reactor utilizing past experimental results to study this process in detail and under

various boundary conditions. A parametric study is conducted to investigate different effective parameters during this process and the influence of each parameter is discussed and compared, so that an efficient discharging process can be estimated.

2. Governing Equations

2.1. Adsorption Model

In the adsorption process, a function of the temperature of the adsorbent and the partial pressure of the adsorbate is applied to describe the amount of adsorbate adsorbed onto the surface of an adsorbent. In this study, Dubinin's theory is used to calculate the equilibrium loading [17]. The basic fact of this theory is that when the size of pores is less than 2 nm, the micropore volume is the decisive factor for the adsorbed amount, not the surface area of the micropores. The calculation of adsorbed volume is done with the following equation [18]:

$$W = W_0 \exp\left[-(A/E)^n\right] \tag{1}$$

where W is the volume of water adsorbed per unit mass of zeolite and W_0 is the maximum volumetric adsorption capacity of the adsorbent, n represents the heterogeneity factor of the micropore size distribution, E is the characteristic energy, which is a value for the adsorption forces between adsorbate and adsorbent. A is the adsorption potential and can be calculated as:

$$A = R_w T \ln\left(\frac{p_s}{p_w}\right) \tag{2}$$

In the above equation, R_w is the adsorbate specific gas constant, p_s is the saturation vapor pressure of the adsorbate at the temperature T, and p_w is the equilibrium pressure of the adsorbate. Here, the volumetric loading can be converted to mass-related loading, X using the density of the adsorbed phase, $\rho(T)$:

$$X = \rho(T)\, W \tag{3}$$

The density of adsorbed water can be expressed as a function of temperature:

$$\rho(T) = \frac{\rho_{20^\circ\mathrm{C}}}{1 + \beta_{20^\circ\mathrm{C}}(T - 293.15K)} \tag{4}$$

where $\rho_{20^\circ\mathrm{C}}$ is the density and $\beta_{20^\circ\mathrm{C}}$ is the thermal expansion coefficient of adsorbate at 20 °C.

The following relationship for the equilibrium loading can be specified from Equations (3) and (4):

$$X^* = \rho(T)\, W_0 \, \exp\left[-(A/E)^n\right] \tag{5}$$

2.2. Adsorption Rate

For the modeling of the adsorption rate, a linear driving force (LDF) model, has been utilized [19].

$$\frac{\partial X}{\partial t} = k_{LDF}[X^* - X] \tag{6}$$

$$k_{LDF} = \frac{15\delta_{eff}}{R_p^2} \tag{7}$$

In the above equations, X is the amount of adsorbed adsorbate and X^* represents the equilibrium adsorption capacity which is the mass of the adsorbed adsorbate to the dry sorbent mass at equilibrium condition. R_p is the average radius of the zeolite beads and δ_{eff} is the effective diffusion coefficient which can be calculated by applying Equation (8) [20].

$$\delta_{eff} = \frac{D_{ges}/\mu}{1 + \alpha(x)} \tag{8}$$

$$\alpha(x) = \frac{\rho_s RT}{\varepsilon_p M_{ads}} \frac{\partial X^*}{\partial p_w} \tag{9}$$

where μ is the tortuosity factor, M_{ads} is the molar mass of water, ε_p is the internal porosity of zeolite particles and $\frac{\partial X^*}{\partial p_w}$ is the slope of the adsorption isotherm. The total diffusion resistance D_{ges} is defined according to the following formula [21]:

$$D_{ges} = \left[1/D_{Kn} + 1/D_{i,j} \right]^{-1} \tag{10}$$

where D_{Kn} is the diffusion resistance of Knudsen Diffusion and $D_{i,j}$ is the diffusion resistance of the free gas diffusion with the gas components i and j. D_{Kn} and $D_{i,j}$ are defined as follows [22]:

$$D_{kn} = \frac{4}{3} d_{pm} \sqrt{\frac{RT}{2\pi M_{ads}}} \tag{11}$$

$$D_{i,j} = \frac{1.013 \times T^{1.75} \times 10^{-7} \left[\frac{1}{M_i} + \frac{1}{M_j} \right]^{1/2}}{p \left[(\sum v_i)^{1/3} + (\sum v_j)^{1/3} \right]^2} \tag{12}$$

where, M_i and M_j represent molar masses in kg/kmol. $\sum v_i$ and $\sum v_j$ are the diffusion volumes of the molecules.

2.3. Adsorption Enthalpy

The adsorption enthalpy is defined as the summation of the vaporization enthalpy, ΔH_v, and binding enthalpy. The following formula gives the adsorption enthalpy of zeolite ΔH, as a function of mass loading X, [18]:

$$-\Delta H_{ads} = \Delta H_v + E \left(\ln \frac{W_0}{W} \right)^{1/n} + \frac{E\beta T}{n} \left(\ln \frac{W_0}{W} \right)^{-(n-1)/n} \tag{13}$$

2.4. Mass and Energy Balance

The continuity equation for air and zeolite particles (porous bed) can be expressed as below [23]:

$$\varepsilon \frac{\partial x_v}{\partial t} = D_{ax} \frac{\partial^2 x_v}{\partial z^2} - v \frac{\partial x_v}{\partial z} + (1-\varepsilon) \frac{\rho_s}{\rho_f} \frac{\partial X}{\partial t} \tag{14}$$

where D_{ax} is the effective axial dispersion, x_v is the water vapor content of the air, ε is the porosity of the bed, and ρ_f and ρ_S are the density of fluid and zeolite bed, respectively.

The following equation can be used to describe the heat transport in the reactor considering the effects of diffusion and convection and with the assumption of constant fluid density [22]. A source is added to the energy equation as a result of the adsorption phenomenon.

$$\begin{aligned} &\left[\varepsilon \rho_f c_{p,f} + \rho_s (1-\varepsilon) \left(c_{p,s} + x_s c_{p,ads} \right) \right] \frac{\partial T}{\partial t} = \frac{\partial}{\partial z} \Lambda_{ax} \frac{\partial T}{\partial z} \\ &- v \rho_f \left(c_{p,f} \frac{\partial T}{\partial z} \right) + \rho_s (1-\varepsilon) \frac{\partial}{\partial t} (\Delta h_{ads} X) - Q_{ambient} \end{aligned} \tag{15}$$

where $c_{p,d}$, $c_{p,ads}$, $c_{p,s}$, and $c_{p,f}$ are the specific heat capacity of the water vapor, adsorbed water, solid, and fluid, respectively, and Λ_{ax} is the effective axial thermal conductivity. $Q_{ambient}$ is the heat exchange at the reactor wall with the ambient.

3. Materials and Methods

The concept behind thermochemical energy storage is the sorption/desorption of a sorbate from a sorbent. In summer, heat at a high temperature (up to 180 °C) required for the desorption (charging) process is provided. During this process, the saturated sorbent in the reactor is dried. Consequently, the sorbate is released in the gaseous state and flows out

of the reactor. During the discharge process, the air containing water vapor flows into the reactor and through the reaction with the unsaturated sorbent, the adsorption enthalpy is released and used for heating applications.

3.1. Physical Model

The fixed-bed reactor that is studied in the current work was previously developed and tested in [22] for an open thermochemical energy storage system. The properties of the binder-free zeolite which is used in the present code are listed in Table 1. A schematic of the reactor is shown in Figure 1 and the geometrical parameters are presented in Table 2. The air containing water vapor flows into the reactor during the adsorption process and after reaction with zeolite leaves the reactor. In this exothermic reaction, the heat will be released, which is taken away by air and can be used for heating applications.

Table 1. Properties of zeolite bed used in the model [22].

Parameter	Value
Maximum adsorption capacity of zeolite (mL/g)	0.27
Characteristic energy (J/kg)	1192.250
Heterogeneity factor (-)	1.55
Bulk density (kg/m^3)	690
Average diameter of zeolite particles/beads (mm)	2
Porosity of desorption bed (-)	0.4
Thermal conductivity of zeolite-13X (W/mK)	0.4
Heat Capacity of zeolite-13X (J/K)	880
Internal porosity of the particle (-)	0.6
Macropore diameter (m)	3×10^{-7}
Tortuosity (-)	4

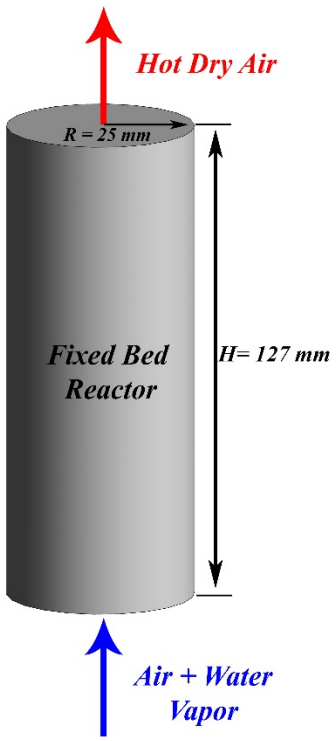

Figure 1. Schematic of the studied reactor.

Table 2. Geometrical parameters of the fix bed reactor [22].

Parameter	Value
Height of the Reactor (mm)	127
Diameter of the reactor (mm)	50
Reactor volume (mL)	250

3.2. Numerical Method

A FORTRAN code was developed for solving the present problem. The following method is used to obtain the temperature and water loading of the zeolite at each point:

The mass and energy equations are discretized and the algebraic equations are transformed into a tridiagonal matrix applying the implicit method and solved using the Thomas algorithm. The velocity is assumed to be uniform over the entire domain, leading to a significant decrease in the computational time, while accurate results can be obtained.

The states of zeolite beads and airflow are described as a function of time and position using the proposed model. The following assumptions are taken into account to develop the numerical model:

- The size, shape, and porosity of particles are assumed to be uniform;
- The air is considered to be an ideal gas (dry air + water vapor);
- The adsorbed water is assumed to be a liquid and in chemical and thermal equilibrium with zeolite;
- The work done by viscous dissipation, radiative heat transfer, and pressure changes is neglected.

Based on the above assumptions, the model can be simplified into a one-dimensional model. Moreover, a heat transfer coefficient value of 1.4 W/(m^2 K) is considered at the sidewall of the fixed bed based on the results provided by Mette et al. [22].

3.3. Definition of the Boundary Conditions

The boundary conditions are considered as follows:

- The temperature of the flow at the inlet is constant and equal to the environment temperature;
- The inlet loading of water in the air is constant and can be calculated based on the relative humidity or partial pressure of the water;
- The flow velocity at the inlet is constant and its direction is normal to the inlet surface;
- Neumann boundary condition is considered at the outlet for temperature and the loading of water in the air.

3.4. Validation of the Developed Code

In order to confirm the accuracy of the developed code, the outputs are compared with the results of previous experiments in the literature. The experimental setup, which was used by Mette et al. [22], uses a fixed-bed reactor made of stainless steel and has an inner diameter of 50 mm, a height of 127 mm, and a wall thickness of 3 mm. It is filled with Binder-free zeolite 13X zeolite particles. Moreover, 80 mm of mineral wool was considered for the insulation of the reactor. During the experiments, the air passes through an oil separator and air dryer, and then a mass flow of 1 kg/h with an accuracy of $\pm$1.4 % was set for the compressed air using a mass flow controller. After passing, the airflow was separated, passed through the humidifier partially, and then recombined. The required humidity was adjusted by regulating the bypass flow utilizing a control valve. The humidified air was heated up to the desired temperature and then flows into the reactor and the adsorption process takes place inside the reactor. The heat released during this process heats up the airflow so that the air leaves the reactor at a higher temperature. The humidity of the air was determined at the inlet and also outlet by measuring the dew point temperature. The air temperature at different heights is measured with the installed thermocouples.

The results of simulations for temperature outlet and adsorption enthalpy are compared with the results presented by Mette et al. [22]. As illustrated in Figure 2, there is good agreement between the outputs of the present study and available experimental data for the case at an adsorption temperature of 30 °C and partial pressure of 15 mbar, which proves the high accuracy of the numerical model.

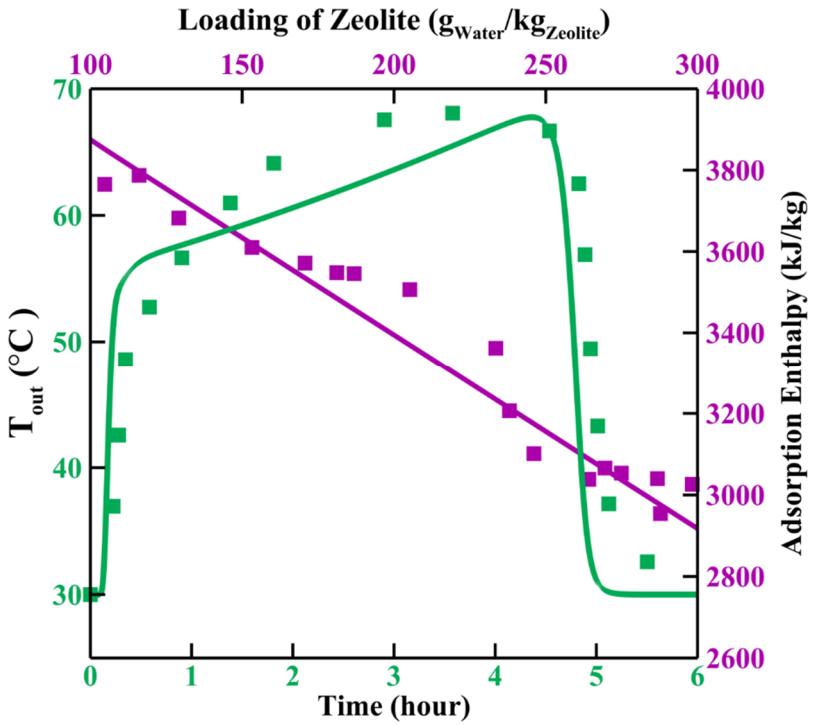

Figure 2. Validation of developed code at T_{ads} = 30 °C and partial pressure of water vapor at 15 mbar.

4. Results and Discussion

In the current investigation, a CFD code was developed to model the adsorption process between zeolite and water for seasonal storage purposes. The effect of desorption temperature, humidity, and mass flow rate of the incoming air on the reaction is studied. The following section discusses the results considering different ranges for input parameters. The influence of desorption temperature and partial pressure on the outlet temperature is discussed and also a parametric study is presented to investigate the influence of input parameters on the discharging time and adsorption enthalpy. In this study, the discharging time is considered as the time from the beginning of the adsorption process until there is no longer any change in the humidity of the outlet air which indicates that the zeolite is completely saturated.

The reaction rate between zeolite and water can be defined using the following equation:

$$v^0 = \frac{0.001\rho_{s,b}}{M_{ads}} \frac{\partial X}{\partial t} \tag{16}$$

where $\rho_{s,b}$ is the bulk density of zeolite.

The value of the reaction rate during the adsorption process is plotted in Figure 3 for the case of $P_{w,ads}$ of 15 mbar and adsorption temperature of 30 °C as shown in Figure 3. As can be observed, the reaction occurs in short time periods, shaping the reaction zone with narrow intervals, due to the high reaction rate of zeolite, and when the zeolite in the reaction zone is saturated, this reaction zone moves forward. Moreover, as time passes, the amplitude of the reaction rate decreases slightly, which is due to the fact that the upstream points have absorbed a small amount of water vapor, which causes the maximum amount of reaction rate for these points to be slightly lower.

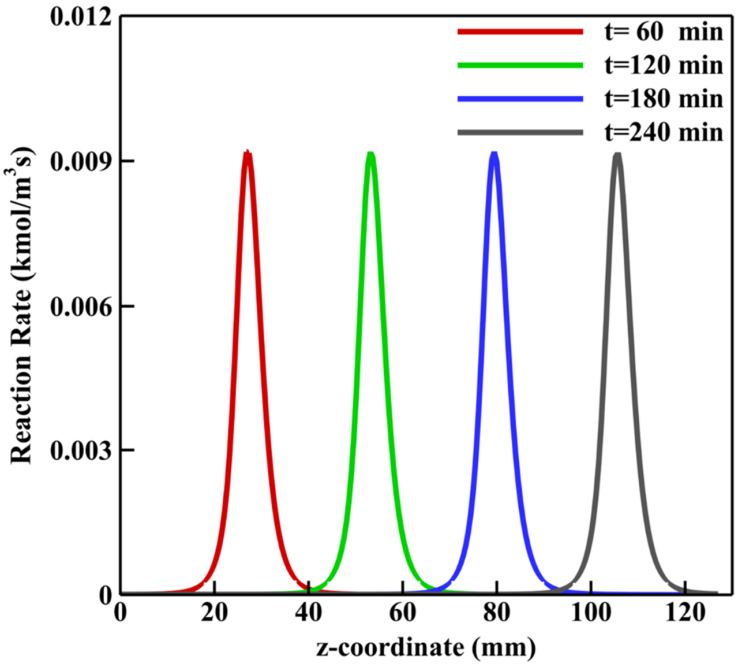

Figure 3. The rate of reaction between zeolite and water along the reactor axis.

The temperature provided during desorption, T_{des}, has a great influence on the stored energy in the sorbent, and consequently the released energy in the adsorption process. This is especially important for heating applications where hot air above some specific temperatures should be provided for the desired time period. Having knowledge about the parameters influencing the outlet temperature and discharging time can be extremely helpful to adjust them in the most efficient way.

To study the influence of this temperature, simulations are conducted at four different charging temperatures of 100, 140, 180, and 220 °C, and the results are presented in Figure 4.

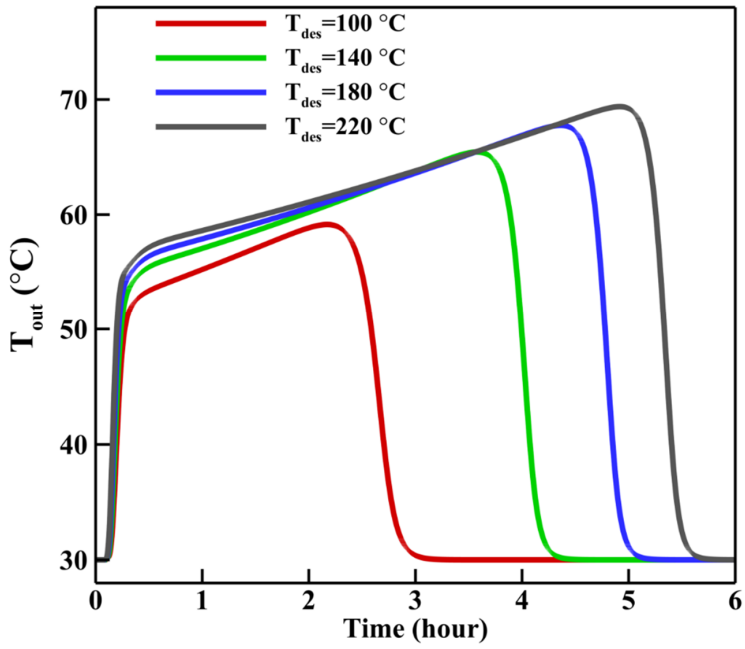

Figure 4. The outlet temperature of the reactor for different desorption temperatures.

To compare the results from different cases better, assume that an outlet temperature of 60 °C (the temperate provided by a conventional heating system for buildings) is needed at the outlet of the system. Based on the simulation results, in the same adsorption temperature of 30 °C and partial pressure of 15 mbar, a maximum achieved outlet temperature, $T_{o,max}$ is equal to 59.14 °C in the case with a T_{des} of 100 °C. For T_{des} of 140 °C, the highest temperature of 65 °C can be provided at the outlet with the possibility of supplying a temperature higher than 60 °C for 117 min. For the case of 180 °C, the maximum achieved temperature is equal to 68 °C and the system can provide the outlet temperature, T_o, higher than 60 °C for a time period of about 174 min. A maximum outlet temperature of 69 °C, and a duration of 221 min above 60 °C can be achieved for cases with T_{des} of 220 °C.

As predicted, when a higher temperature is provided during the desorption process, a higher outlet temperature for a longer time period can be achieved, showing the importance of the desorption temperature; however, there is no linear relationship between the desorption temperature and the maximum achieved temperature in the adsorption process.

The comparison of the released adsorption enthalpy also shows that the system is highly sensitive to the desorption temperature, which is because of the fact that at higher T_{des}, less water exists in the zeolite at the end of the desorption process, so more capacity is available during discharging. Another important parameter that influences the reaction between zeolite and water is the partial pressure of water vapor, $p_{w,ads}$, which is an indicator of the incoming air humidity. As can be clearly observed in Figure 5, the released energy from zeolite increases significantly with increasing the partial pressure. The reason is increasing available water vapor that can react with zeolite, leading to higher outlet temperature. However, the discharge time decreases because the zeolite becomes saturated sooner.

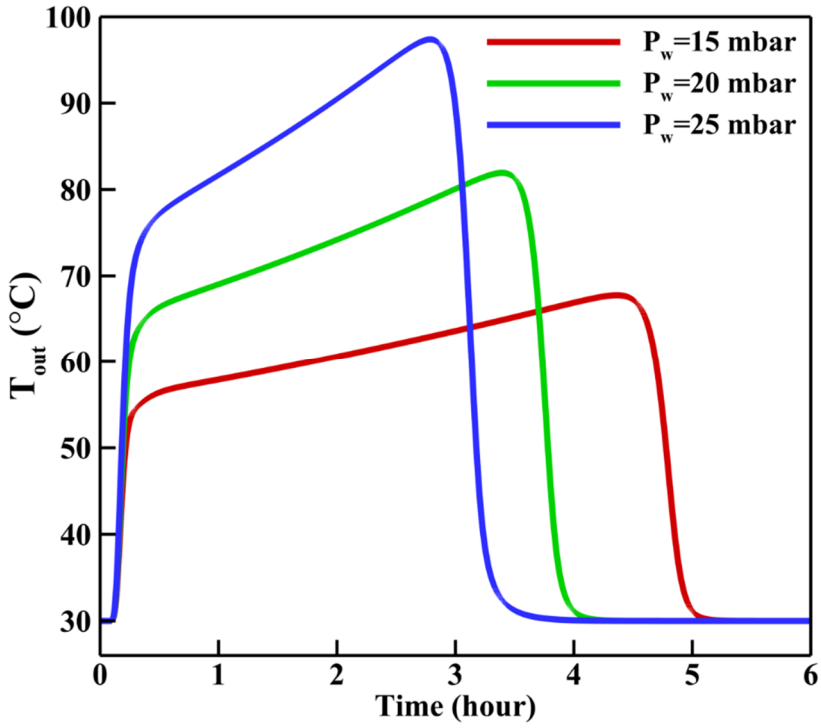

Figure 5. Variation of outlet temperature under different $p_{w,in}$.

To study the influence of the mass flow rate (MFR) of the incoming air on the discharging process, three different values—1, 1.5, and 2 kg/h—are considered for mass flow rate and the variations of discharging time, outlet temperature, and released adsorption enthalpy are calculated.

As can be clearly seen in Figure 6, this parameter has a significant effect on the discharging time; with increasing MFR, the reaction between water and zeolite occurs faster. However, there is no significant influence on $T_{o,max}$.

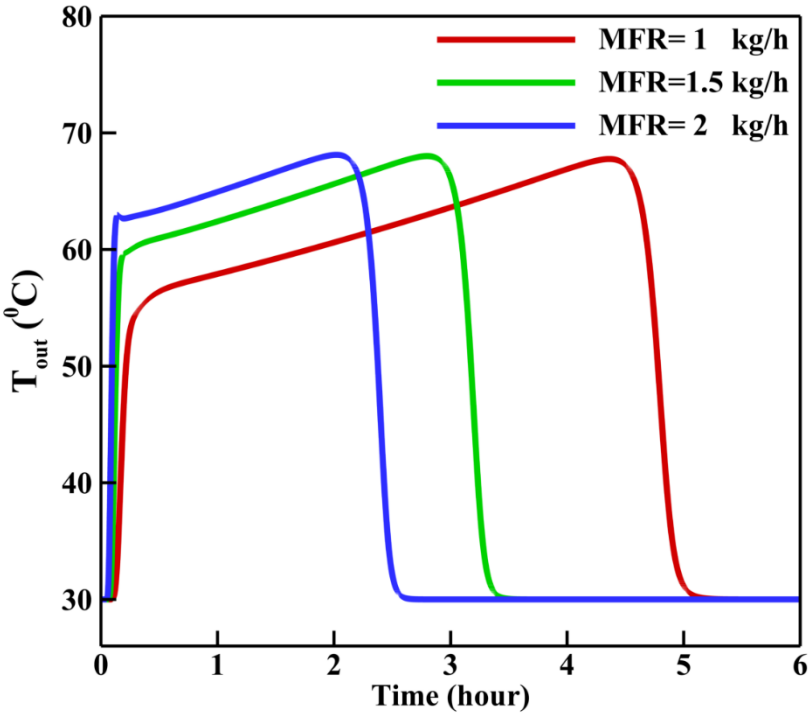

Figure 6. Outlet temperature under a different mass flow rate of incoming air at partial pressure of 15 mbar.

The cases with MFRs of 1, 1.5, and 2 kg/h have the maximum achievable temperatures of 67.7 °C, 68 °C, and 68.1 °C, respectively, but the duration with a temperature above 60 °C is equal to 174 min, 170 min, and 131 min, respectively, showing that with increasing mass flow rate, outlet temperature higher than 60 °C can be achieved for a shorter period of time.

To interpret the influence of different factors on the process of adsorption of zeolite/water pairs, three decisive parameters of desorption temperature (T_{des}), partial pressure of water vapor ($P_{w,ads}$), and air mass flow rate (MFR) are considered, and changing of mean adsorption enthalpy, discharging time, and amount of adsorbed water in adsorption process are also considered. Desorption temperature is the temperature provided during the charging process. To involve this parameter in the study, the amount of water loading of zeolite after the desorption process under the charging temperature is read from the zeolite isotherms based on the Dubinin equation and imported as the initial loading of zeolite at the beginning of the adsorption process. To have the same condition for all simulations, the partial pressure during the desorption process is considered equal to 10 mbar for all cases. A range between 120–180 °C is taken into account for desorption temperatures and the impact of this parameter on the adsorption process of zeolite/water is studied. The other parameter of interest is the partial pressure of water vapor in the inlet during the adsorption process. For numerical study, values between 5–25 mbar are considered for this parameter. The other studied parameter is the mass flow rate of air valued between 0.5–2 kg/h. Considering these ranges, several simulations are conducted to study the influence of these parameters on adsorption mean specific enthalpy, amount of adsorbed water during adsorption, and time to complete the adsorption process.

The released enthalpy during the adsorption process is represented by mean specific adsorption enthalpy $h_{ads,m}$. The influence of T_{des}, $p_{w,ads}$, and MFR on $h_{ads,m}$ are studied, and the results of simulations are illustrated in Figure 7.

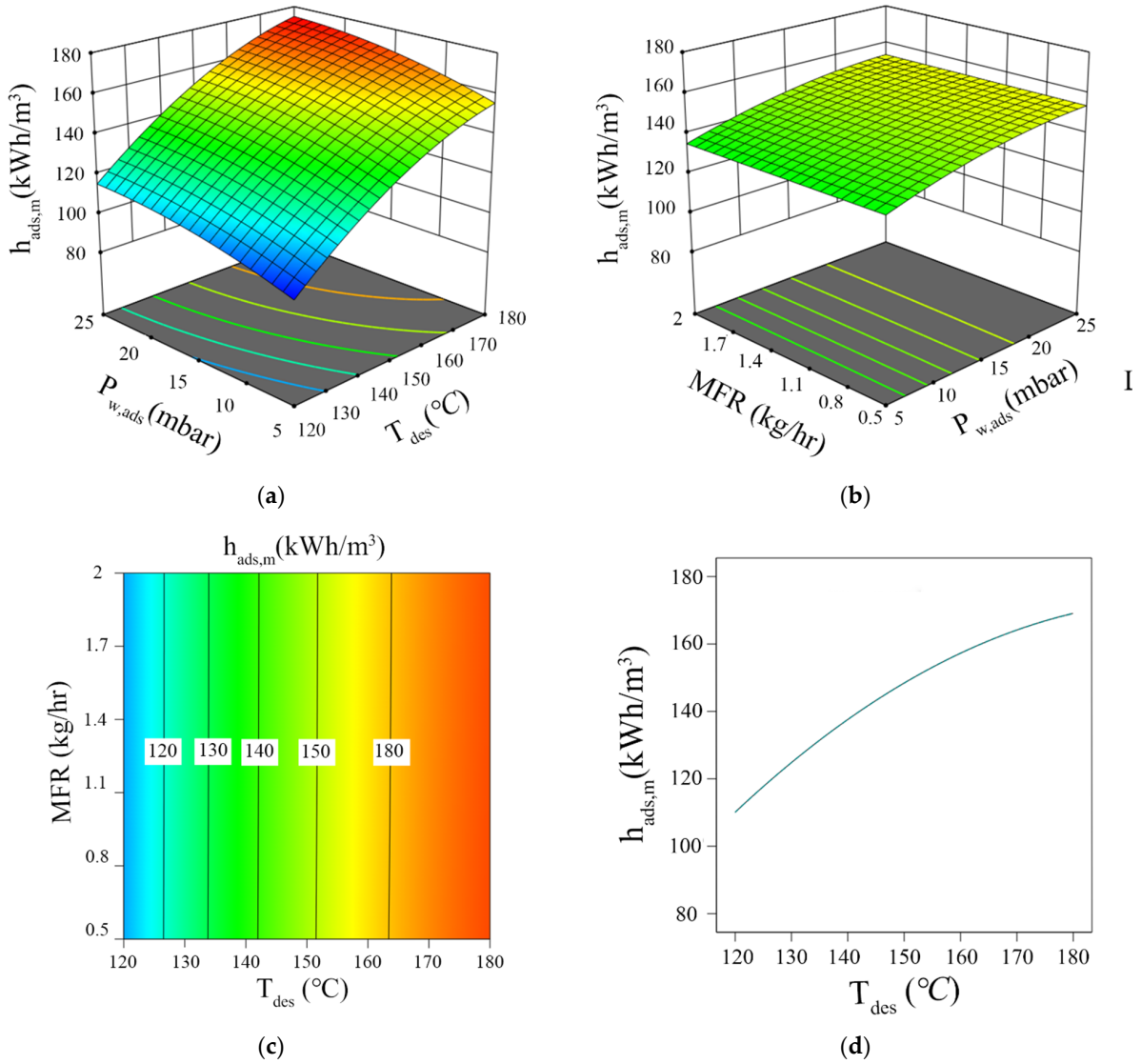

Figure 7. Variation of the mean specific adsorption enthalpy with (**a**) desorption temperature and partial pressure of water vapor (**b**) mass flow rate and partial pressure (**c**) desorption temperature and mass flow rate of the incoming air (**d**) desorption temperature.

As can be seen, higher mean specific adsorption enthalpy $h_{ads,m}$ can be achieved by proving higher desorption temperatures or higher partial pressures, while the mass flow rate has little influence on the amount of the adsorption enthalpy.

Figure 7b shows the changes of $h_{ads,m}$ under different partial pressures and mass flow rates at a desorption temperature of 150 °C, and Figure 7d shows the variation of $h_{ads,m}$ with T_{des} for the case with an MFR of 1 kg/h and partial pressure of 15 mbar. At lower desorption temperatures, more water remains inside the zeolite, and due to higher loading, the interaction between the adsorptive decreases, and the bonding forces also decrease, leading to a reduction in adsorption enthalpy.

For the considered parameters, an equation in terms of coded factors can be utilized to make predictions about the response. The relative influence of each parameter can be identified using the code by comparing the factor coefficients. Changes of $h_{ads,m}$ according to relevant parameters can present the following mathematical relationship.

$$\begin{aligned} h_{ads,m} &= 148.39 + 29.49T_{des} + 9.29P_{w,ads} - 0.1240MFR + 0.23T_{des}P_{w,ads} \\ &-0.08T_{des}MFR - 0.0555P_{w,ads}MFR - 8.82(T_{des})^2 - 3.83(P_{w,ads})^2 \\ &+0.035(MFR)^2 \end{aligned} \quad (17)$$

This relationship also emphasizes the great importance of desorption temperature on the released energy during adsorption. However, it can be seen that partial pressure also has a somehow important effect on the adsorption enthalpy, which means that if, for example, a very high temperature cannot be provided during desorption, this can be compensated to some extent by providing higher moisture.

The variation of discharging time with changing desorption temperature, partial pressure, and incoming mass flow rate is investigated and presented in Figure 8. It appears that the mass flow rate of the incoming air has a great potential to influence the discharging time. This time also increases with increasing charging temperatures because in higher T_{des} there is less loading inside the zeolite, and under constant partial pressure more time is required for saturation. By augmenting the partial pressure of water vapor, the amount of water entering the reactor increases, so the reaction rate rises, and the reaction occurs faster and causes the reactor to discharge faster.

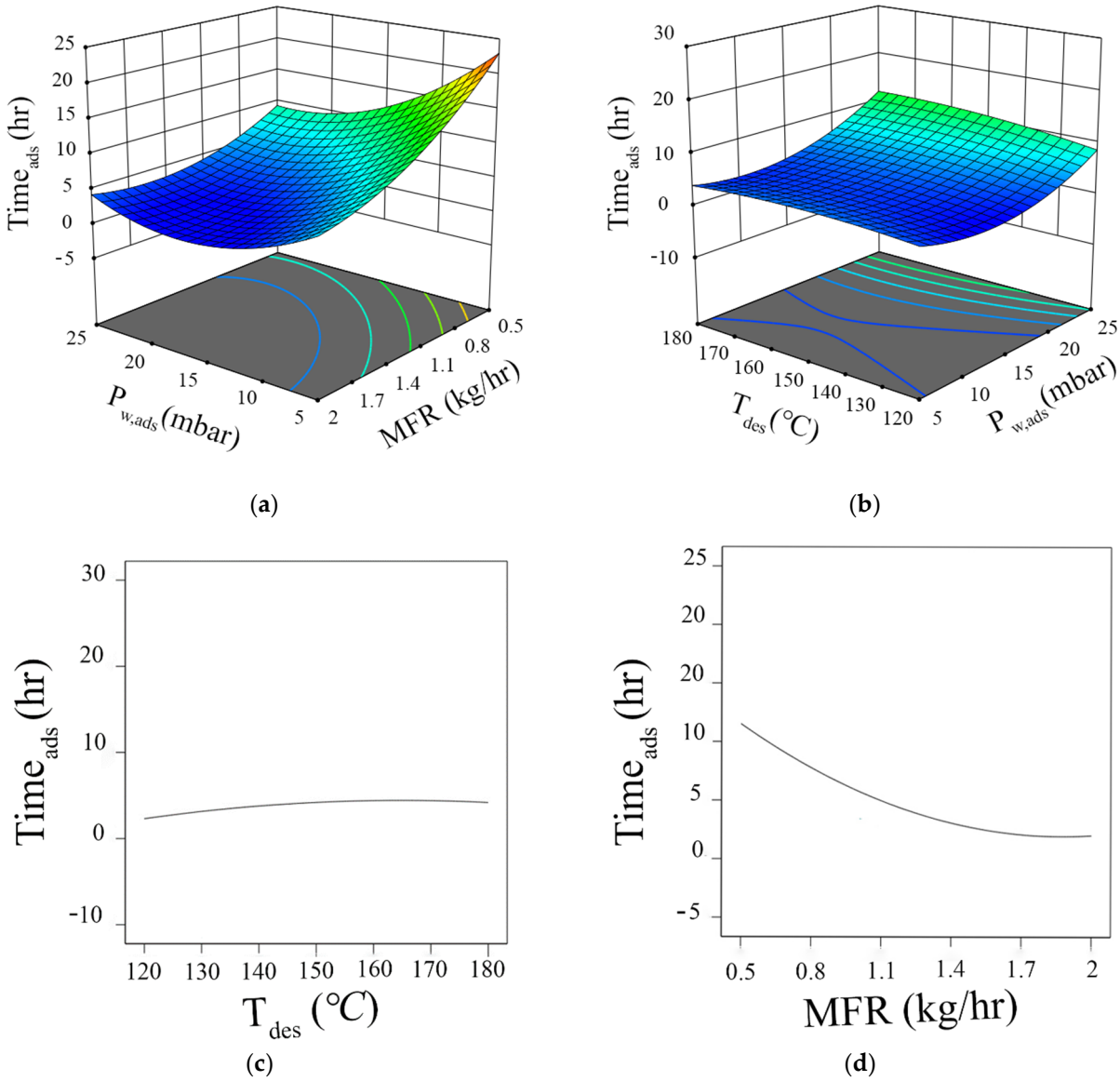

Figure 8. The influence of (**a**) mass flow rate and partial pressure (**b**) desorption temperature and partial pressure (**c**) desorption temperature and (**d**) mass flow rate of incoming air on the discharging time of the reactor.

The changes of discharging time according to relevant parameters are presented in Figure 8, and Equation (18) can present the following associations.

$$Time_{ads} = 3.92 + 0.88T_{des} - 3.23P_{w,ads} - 4.76MFR - 0.8T_{des}P_{w,ads} \\ -0.56T_{des}MFR + 2.77P_{w,ads}MFR - 0.95(T_{des})^2 + 4.16(P_{w,ads})^2 \\ +2.86(MFR)^2 \quad (18)$$

The influence of the partial pressure and temperature during the desorption on the adsorbed amount of water was investigated. Based on the results, presented in Figure 9, a much higher temperature is provided in the desorption process, and the higher the partial pressure of the water vapor, the greater the capacity of the zeolite to absorb water, which means more sorption storage density and released energy. However, the mass flow rate has a negligible influence on the amount of adsorbed water.

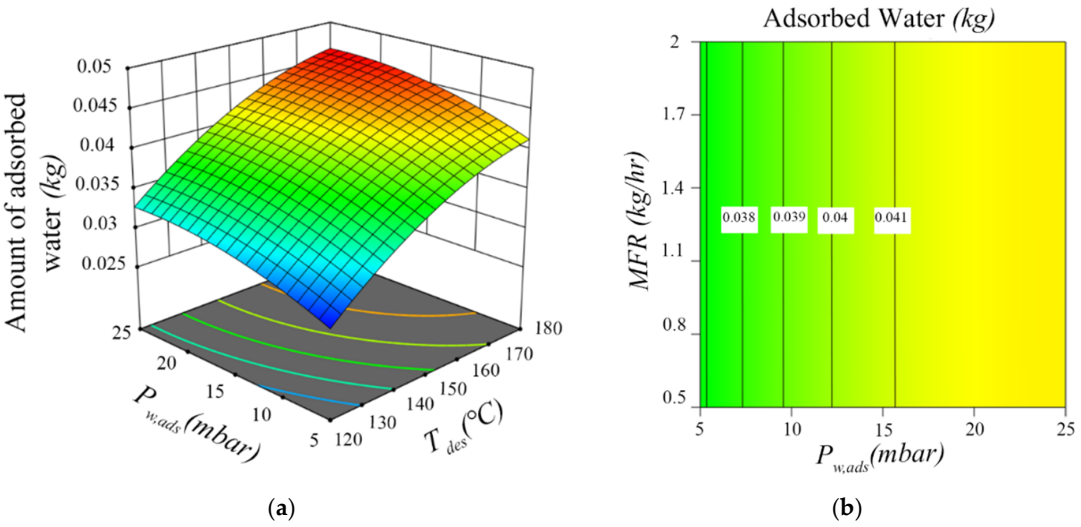

(**a**) (**b**)

Figure 9. Amount of adsorbed water under different (**a**) desorption temperatures and partial pressures (**b**) mass flow rates and partial pressures.

Variations of adsorbed water amount in terms of the coded factors can be represented using the following mathematical relationship.

$$Amount\ of\ adsorbed\ water = 0.0408 + 0.007T_{des} + 0.0026P_{w,ads} + 2.57 \times 10^{-6}MFR \\ -1.001 \times 10^{-6}T_{des}P_{w,ads} - 1.41 \times 10^{-6}T_{des}MFR + 3.64 \times 10^{-6}P_{w,ads}MFR - 0.0023(T_{des})^2 \\ +0.0014(P_{w,ads})^2 - 1.89 \times 10^{-6}(MFR)^2 \quad (19)$$

Based on the above equation, the desorption temperature has the highest influence on the amount of adsorbed water, which also leads to higher amounts of released energy.

5. Conclusions and Outlook

To better interpret the ongoing processes in thermochemical reactors for seasonal heat storage, a mathematical model is developed in the present study to simulate the dynamic adsorption process of zeolite 13X and water in a fixed-bed reactor. Experimental data were used to validate and approve the accuracy of the developed code. After the validation, several parameters and their influence on the adsorption process were studied. The aim was to determine to what extent these parameters can influence the adsorption reaction. The simulation results show that the narrow zone in which the adsorption reaction takes place is striking, which is due to the very fast kinetics. The parametric study considering desorption temperature, incoming air mass flow rate, and partial pressure of water vapor also reveals that the output temperature of the reactor is directly dependent on desorption temperature and air humidity, while the discharging time is mostly affected by the mass flow rate and humidity of the air. Under higher desorption temperatures, the amount of

water in zeolite is lower, providing a greater capacity for adsorbing water and leading to higher released enthalpy, while a higher partial pressure means there is more available water in the incoming air, which increases the reaction rate between zeolite and water, so a higher outlet temperature and release heat is possible.

The model developed in the current study has provided the opportunity of investigating different parameters involved in the adsorption process in detail. In future studies, this model will be extended to be integrated into a thermodynamic cycle including a solar collector, and the behavior of a scaled reactor during adsorption and desorption will be studied.

Author Contributions: Conceptualization, E.A. and G.F.; Methodology, E.A. and G.F.; Software, E.A.; Supervision, G.F.; Validation, E.A.; Visualization, E.A.; Writing—original draft, E.A. and G.F.; Writing—review & editing, G.F. All authors have read and agreed to the published version of the manuscript.

Funding: This work was supported by the Saarland State Ministry for Finance and Science (Department W/2).

Institutional Review Board Statement: Not applicable.

Informed Consent Statement: Not applicable.

Data Availability Statement: Not applicable.

Conflicts of Interest: The authors declare no conflict of interest.

Nomenclature

A	Area [m^2]
A	Adsorption potential [J/kg]
C_p	Heat Capacity
E	Characteristic energy [kJ/kg]
D	Dispersion coefficient [m^2/s]
D_{ges}	Total diffusion coefficient [m^2/s]
D_{kn}	Knudsen diffusion coefficient [m^2/s]
$D_{i,j}$	Free gas diffusion coefficient [m^2/s]
E	Characteristic energy [kJ/kg]
n	Heterogeneity factor [-]
p	Pressure [Pa]
p_s	Saturation vapor pressure [Pa]
p_w	Water vapor partial pressure [Pa]
R_p	Average radius of zeolite particles/beads
R_w	Specific gas constant of water vapor [kJ/kg]
T	Temperature [K]
W	Adsorption volume [mol/g]
W_0	Maximum adsorption capacity of zeolite [mol/g]
X^*	Equilibrium loading [-]
Greek symbols	
ρ	Density [kg/m^3]
$\rho_{20°C}$	Adsorbate density at 20 °C [kg/m^3]
β	Thermal expansion coefficient [1/K]
δ_{eff}	Diffusion coefficient
μ	Tortuosity factor
Λ_{ax}	Axial thermal conductivity
ε	porosity [-]
Subscripts	
ads	adsorption
des	desorption
ax	axial

References

1. Moon, W.C. A review on interesting properties of chicken feather as low-cost adsorbent. *Int. J. Integr. Eng.* **2019**, *11*, 136–146. [CrossRef]
2. Tatsidjodoung, P.; Le Pierrès, N.; Luo, L. A review of potential materials for thermal energy storage in building applications. *Renew. Sustain. Energy Rev.* **2013**, *18*, 327–349. [CrossRef]
3. Zheng, X.; Ge, T.S.; Wang, R.Z. Recent progress on desiccant materials for solid desiccant cooling systems. *Energy* **2014**, *74*, 280–294. [CrossRef]
4. Thompson, R.W. Recent advances in the understanding of zeolite synthesis. *Synthesis* **1998**, *74*, 280–294.
5. Zhang, Y.; Wang, R. Sorption thermal energy storage: Concept, process, applications and perspectives. *Energy Storage Mater.* **2020**, *27*, 352–369. [CrossRef]
6. Hirasawa, Y.; Urakami, W. Study on specific heat of water adsorbed in Zeolite using DSC. *Int. J. Thermophys.* **2010**, *31*, 2004–2009. [CrossRef]
7. Lu, Y.Z.; Wang, R.Z.; Zhang, M.; Jiangzhou, S. Adsorption cold storage system with zeolite–water working pair used for locomotive air conditioning. *Energy Convers. Manag.* **2003**, *44*, 1733–1743. [CrossRef]
8. Wang, L.W.; Wang, R.Z.; Oliveira, R.G. A review on adsorption working pairs for refrigeration. *Renew. Sustain. Energy Rev.* **2009**, *13*, 518–534. [CrossRef]
9. Engel, G.; Asenbeck, S.; Koell, R.; Kerskes, H.; Wagner, W.; van Helden, W. Simulation of a seasonal, solar-driven sorption storage heating system. *J. Energy Storage* **2017**, *13*, 40–47. [CrossRef]
10. Wang, D.C.; Xia, Z.Z.; Wu, J.Y. Design and performance prediction of a novel zeolite–water adsorption air conditioner. *Energy Convers. Manag.* **2006**, *47*, 590–610. [CrossRef]
11. Vasta, S.; Freni, A.; Sapienza, A.; Costa, F.; Restuccia, G. Development and lab-test of a mobile adsorption air-conditioner. *Int. J. Refrig.* **2012**, *35*, 701–708. [CrossRef]
12. Bales, C.; Gantenbein, P.; Jaenig, D.; Kerskes, H.; Summer, K.; van Essen, M.; Weber, R. *Laboratory Tests of Chemical Reactions and Prototype Sorption Storage Units*; A Report of IEA Solar Heating and Cooling Programme-Task; IEA-SHC: Paris, France, 2008; Volume 32.
13. Jähnig, D.; Hausner, R.; Wagner, W.; Isaksson, C. Thermo-chemical storage for solar space heating in a single-family house. In Proceedings of the Ecostock, Galloway, NJ, USA, 31 May–2 June 2006.
14. Hongois, S.; Kuznik, F.; Stevens, P.; Roux, J.-J. Development and characterisation of a new $MgSO_4{}^-$ zeolite composite for long-term thermal energy storage. *Sol. Energy Mater. Sol. Cells* **2011**, *95*, 1831–1837. [CrossRef]
15. Köll, R.; Van Helden, W.; Engel, G.; Wagner, W.; Dang, B.; Jänchen, J.; Kerskes, H.; Badenhop, T.; Herzog, T. An experimental investigation of a realistic-scale seasonal solar adsorption storage system for buildings. *Sol. Energy* **2017**, *155*, 388–397. [CrossRef]
16. Jänchen, J.; Herzog, T.H.; Gleichmann, K.; Unger, B.; Brandt, A.; Fischer, G.; Richter, H. Performance of an open thermal adsorption storage system with Linde type A zeolites: Beads versus honeycombs. *Microporous Mesoporous Mater.* **2015**, *207*, 179–184. [CrossRef]
17. Bering, B.P.; Dubinin, M.M.; Serpinsky, V.V. Theory of volume filling for vapor adsorption. *J. Colloid Interface Sci.* **1966**, *21*, 378–393. [CrossRef]
18. Do, D.D. *Adsorption Analysis: Equilibria and Kinetics (with cd Containing Computer MATLAB Programs)*; World Scientific: Singapore, 1998; Volume 2.
19. Glueckauf, E. Theory of chromatography. Part 10.—Formulæ for diffusion into spheres and their application to chromatography. *Trans. Faraday Soc.* **1955**, *51*, 1540–1551. [CrossRef]
20. Kast, W. Adsorption aus der Gasphase. In *Ingenieurwissenschaftliche Grundlagen und Technische Verfahren*; Verlag Chemie: Weinheim, Germany, 1988.
21. Bathen, D.; Breitbach, M. Einführung in die Adsorptionstechnik. In *Adsorptionstechnik*; Springer: Berlin/Heidelberg, Germany, 2001; pp. 1–11.
22. Mette, B. *Experimentelle und Numerische Untersuchungen zur Reaktionsführung Thermochemischer Energiespeicher*; University of Stuttgart: Stuttgart, Germany, 2014.
23. Solmuş, İ.; Rees, D.A.S.; Yamalı, C.; Baker, D.; Kaftanoğlu, B. Numerical investigation of coupled heat and mass transfer inside the adsorbent bed of an adsorption cooling unit. *Int. J. Refrig.* **2012**, *35*, 652–662. [CrossRef]